

lular atrophy and a reduction in the number of mitochondria, exclusively in spiral ligament fibrocytes.^{6,7} In the otospiralin-deficient mouse, degeneration of type II and IV fibrocytes is the main pathological change, and hair cells and the stria vascularis appear normal.³ Furthermore, in mouse and gerbil models of age-related hearing loss,⁸⁻¹⁰ degeneration of the cochlear fibrocytes precede the degeneration of other types of cells within the cochlea, with notable pathological changes seen especially in type II, IV, and V fibrocytes. In humans, mutations in the connexin 26 (*Cx26*) and connexin 30 (*Cx30*) genes, which encode gap junction proteins and are expressed in cochlear fibrocytes and nonsensory epithelial cells, are well known to be responsible for hereditary sensorineural deafness.^{11,12} These instances of deafness related to genetic, structural, and functional alterations in the cochlear fibrocytes highlight the functional importance of these fibrocytes in maintaining normal hearing.

Recently, we developed an animal model of acute sensorineural hearing loss attributable to acute cochlear energy failure by administering the mitochondrial toxin 3-nitropropionic acid (3NP) into the rat round window niche.^{13,14} 3NP is an irreversible inhibitor of succinate dehydrogenase, a complex II enzyme of the mitochondrial electron transport chain.^{15,16} Systemic administration of 3NP has been used to produce selective striatal degeneration in the brain of several mammals.^{17,18} Our model with 3NP administration into the rat cochlea showed acute sensorineural hearing loss and revealed an initial pathological change in the fibrocytes of the lateral wall and spiral limbus without any significant damage to the organ of Corti or spiral ganglion. Furthermore, depending on the dose of 3NP used, these hearing loss model rats exhibited either a permanent threshold shift or a temporary threshold shift. In the present study, we used doses of 3NP that induce temporary threshold shift to explore the mechanism of hearing recovery after injury to the cochlear fibrocytes and examined a novel therapeutic approach to repair the injured area using mesenchymal stem cell (MSC) transplantation.

MSCs are multipotent cells that can be isolated from adult bone marrow and can be induced to differentiate into a variety of tissues *in vitro* and *in vivo*.¹⁹ Human MSCs transplanted into fetal sheep intraperitoneally undergo site-specific differentiation into chondrocytes, adipocytes, myocytes, cardiomyocytes, bone marrow stromal cells, and thymic stroma.²⁰ Furthermore, when MSCs were transplanted into postnatal animals, they could engraft and differentiate into several tissue-specific cell types in response to environmental cues provided by different organs.²¹ These transplantability features of MSCs suggested the possibility that they could restore hearing loss in 3NP-treated rats to the normal range. Recently, experimental bone marrow transplantation into irradiated mice suggested that a part of spiral ligament that consists of cochlear fibrocytes was derived from bone marrow cells or hematopoietic stem cells.²² This indicates that bone marrow-derived stem cells such as MSCs may have a capacity to repair the injury of cochlear fibrocytes. In this study, we demonstrate that MSC transplantation significantly improves hearing recovery, and

present evidence suggesting invasion of transplanted MSCs into the injured region of the cochlear lateral wall and repair of the interrupted gap junction network.

Materials and Methods

Rat Model of Acute Sensorineural Hearing Loss Attributable to Cochlear Fibrocyte-Specific Injury

Experimental procedures reported in this study were approved by the Institutional Animal Care and Use Committee of the National Tokyo Medical Center. Sprague-Dawley rats (Clea Japan, Tokyo, Japan) weighing between 180 and 210 g (8 to 10 weeks old) were used. Before surgery, the animals were anesthetized with pentobarbital (30 to 40 mg/kg, i.p.; Dainippon Pharmaceutical, Osaka, Japan), and after local administration of 1% lidocaine (AstraZeneca PLC, London, UK), an incision was made posterior to the left pinna near the external meatus. The left otic bulla was opened to approach the round window niche. The distal end of a section of PE 10 tubing (Becton-Dickinson, Franklin Lakes, NJ) was drawn to a fine tip in a flame and gently inserted into the round window niche. 3NP (Sigma, St. Louis, MO) was dissolved in saline at 300 mmol/L and the pH adjusted to 7.4 with NaOH. Saline alone was used as a control. The solution was administered for 2 minutes at a rate of 1.5 μ l/minute with a syringe pump. After treatment, a small piece of gelatin was placed on the niche to keep the solution in the niche regardless of head movement, and the wound was closed. The right cochlea was surgically destroyed to avoid cross-hearing during auditory brainstem response (ABR) recording.

Auditory Brainstem Response

ABR recording was performed as previously described¹³ before surgery and at 2 hours and 1, 2, 3, 7, 14, 21, 28, 35, and 42 days after surgery (or until 14 days in the MSC transplantation experiment). Six to 12 rats in each group were used for the recordings. ABR was recorded using Scope waveform storing and stimulus control software and the PowerLab data acquisition and analysis system (PowerLab2/20; AD Instruments, Castle Hill, Australia). Electroencephalogram recording was performed using a digital Bioamp extracellular amplifier system (BAL-1; Tucker-Davis Technologies, Alachua, FL). Sound stimuli were produced by a coupler type speaker (ES1spc; Bio Research Center, Nagoya, Japan) inserted into the ear canal. Pure tone bursts of 8, 20, and 40 kHz (0.2-ms rise/fall time and 1-ms flat segment) were generated, and the amplitude was specified by a real-time processor and programmable attenuator (RP2.1 and PA5; Tucker-Davis Technologies). Sound level calibration and frequency confirmation were performed using a 1/4 inch free-field mic (7016; ACO Pacific, Belmont, CA), microphone amp (MA3; Tucker-Davis Technologies), a digital oscilloscope (DS-8822P; Iwatsu Electronic, Tokyo, Japan), and a sound level meter (NL32; Rion, Tokyo, Japan). The maximum output level was 87, 86, and 96 dB at 8, 20, and 40

kHz, respectively. For recording, the animals were anesthetized with pentobarbital before stainless steel needle electrodes were placed ventrolateral to the ears. Waveforms of 512 stimuli at a frequency of 9 Hz were averaged, and the visual detection threshold was determined by increasing or decreasing the sound pressure level in 5-dB steps. The effects of 3NP and/or MSC transplantation on the ABR threshold and recovery ratio of ABR threshold (peak threshold – threshold at 14 days or 42 days/peak threshold × 100) were statistically analyzed at each frequency using an unpaired Student's *t*-test. The significance level for all statistical procedures was set at $P < 0.05$.

Bromodeoxyuridine (BrdU) Injection

To detect cell proliferation in the rat inner ear, BrdU (Sigma) was injected (30 mg/kg *i.p.* per single injection) as previously described.²³ Injections were started just after 3NP administration and continued every 12 hours for 3 or 6 days.

MSC Preparation

We previously established bone marrow MSCs and demonstrate their potential to differentiate into several cell types.²⁴ The cells were prepared from 6- to 8-week-old male F344 rats (Clea) as described. In brief, surgical treatment was performed after intraperitoneal injection of pentobarbital (30 to 40 mg/kg, *i.p.*). After surgery, the rats were sacrificed by ether inhalation followed by dislocation of the neck. Rat femurs and tibiae were collected and the long bones meticulously dissected to remove all adherent soft tissue. Both ends of the bones were cut away from the diaphyses with bone scissors. The bone marrow plugs were hydrostatically expelled from the bones by inserting 18-gauge needles fastened to 10-ml syringes filled with complete medium [Dulbecco's modified Eagle's medium (Sigma), 10% fetal bovine serum (Sigma), and 100 U/ml penicillin-streptomycin (Sigma)] into the distal ends of the femora and the proximal ends of the tibiae. Cells were plated on plastic culture dishes. The nonadherent cell population was removed after 24 hours, and the adherent layer was washed once with fresh media. The cells were then continuously cultured for 1 to 4 weeks in complete medium. Medium was completely replaced every 3 days. When the cells were nearly confluent, the adherent cells were released from the dishes with 0.25% trypsin-ethylenediaminetetraacetic acid (Sigma), split 1:3, and seeded onto fresh plates. Cells from passages 10 to 15 were stored with Cell Banker reagent (Juji Field, Tokyo, Japan) in liquid nitrogen. The frozen cell suspensions were thawed at 1 week before the transplantation and cultured in complete medium at 37°C in a humidified atmosphere of 5% CO₂. The potential of these cells as MSCs were previously demonstrated as described.²⁴ The surface marker expression of these cells was analyzed by flow cytometry (Epics Altra with HyPerSort cell sorting system; Beckman Coulter, Fullerton, CA). At ~80 to 90% confluence, MSCs were disso-

ciated by treatment with 1× Accutase (Chemicon International, Temecula, CA) for 15 minutes at 37°C followed by phosphate-buffered saline (PBS) washout, centrifugation at 1200 rpm for 10 minutes, and resuspension in Hanks' balanced salt solution (HBSS)⁺ medium [HBSS⁻ medium (Invitrogen Japan, Tokyo, Japan) with 2% fetal bovine serum and 10 mmol/L 2-[4-(2-hydroxyethyl)-1-piperazinyl]ethanesulfonic acid (HEPES) buffer (Invitrogen Japan)]. MSCs were incubated with antibodies against CD45, CD31, CD29, CD44H, CD54, CD73, and CD90 (BD PharMingen, San Diego, CA) for 30 minutes on ice and spun down. At the end of the staining, MSCs were resuspended in ice-cold HBSS⁺ medium containing 2 μg/ml propidium iodide for discrimination of dead cells. To detect the MSCs after injection, cultured MSCs were incubated with 5 μmol/L BrdU for 2 days before transplantation as previously described.²⁵

MSC Transplantation

Before transplantation, cultured MSCs were released from the dishes with 0.25% trypsin-ethylenediaminetetraacetic acid and washed by centrifugation with Dulbecco's phosphate-buffered saline (D-PBS; Invitrogen Japan) and resuspended to prepare MSC suspension (1 × 10⁵ cells in 20 μl of D-PBS) for the following transplantation. Three days after 3NP administration, the rats were anesthetized with pentobarbital (30 to 40 mg/kg, *i.p.*) and by local administration of 1% lidocaine. Incisions were made as described for 3NP administration, the surfaces of the posterior and lateral semicircular canals were exposed, and a small hole was made in each canal. A small tube (Eicom, Kyoto, Japan) was inserted into the lateral semicircular canal toward the ampulla. Through this tube, the perilymph was perfused with an MSC suspension (1 × 10⁵ cells in 20 μl of D-PBS) for 10 minutes at a rate of 2 μl/minute using a syringe pump with drainage from the hole made on the posterior semicircular canal. The tube was then removed, the holes on the semicircular canals were sealed with a muscle and fibrin adhesive (Beriplast P Combi-set; CSL Behring, King of Prussia, PA), and the wound on the neck was closed. An equal volume of vehicle (D-PBS) was also injected into the semicircular canal of 3NP-treated rats as control.

Tissue Preparation

The rats were sacrificed at 3 days (three rats for 3NP and three rats for saline control) and 42 days (five rats for 3NP and three rats for saline control) after 3NP treatment and 11 days after MSC transplantation (12 rats for 3NP with MSC transplantation, seven rats for MSC transplantation only, and five rats for 3NP followed by vehicle injection). They were deeply anesthetized with pentobarbital and transcardially perfused with 0.01 mol/L phosphate buffer, pH 7.4, containing 8.6% sucrose followed by a fixative consisting of freshly depolymerized 4% paraformaldehyde in 0.1 mol/L phosphate buffer (pH 7.4). After decapitation, the left temporal bones were removed and immediately placed in the same fixative. Small openings

were made at the round window, oval window, and the apex of the cochlea. After overnight immersion in fixative, the temporal bones were decalcified by immersion in 5% sucrose, 5% ethylenediaminetetraacetic acid, pH 7.4, with stirring at 4°C for 14 days. The specimens were dehydrated through graded concentrations of alcohol, embedded in paraffin blocks, and sectioned into 5- μ m-thick slices. The sections were stained with hematoxylin and eosin (H&E) as generally described, by terminal deoxynucleotidyl transferase (TdT)-mediated dUTP nick-end labeling (TUNEL) and by immunohistochemistry for BrdU, Cx30, or Cx26 as described below.

TUNEL Assay

TUNEL assays were performed using an ApopTag Fluorescein Direct *in situ* apoptosis detection kit (Chemicon International) according to the manufacturer's instructions. In brief, specimens were digested with 20 μ g/ml proteinase K in 0.01 mol/L PBS, pH 7.4, for 5 minutes, incubated with TdT and fluorescein-labeled nucleotide in a humid atmosphere at 37°C for 1 hour, and then incubated with 2 μ mol/L TOPRO-3 iodide (Molecular Probes, Eugene, OR) for 5 minutes. The specimens were viewed with a confocal laser microscope (LSM510; Carl Zeiss, Esslingen, Germany; or Radiance 2100; Bio-Rad, Hercules, CA), and each image was analyzed and saved by ZeissLSM image browser (Carl Zeiss). Negative controls included proteinase K digestion but did not include TdT so that nonspecific incorporation of nucleotide, or nonspecific binding of enzyme-conjugate, could be assessed. Distilled water was substituted for TdT enzyme reagent in negative controls.

Immunohistochemistry

After pretreatment with 2 mol/L HCl at 37°C for 30 minutes, incubation with 20 μ g/ml proteinase K in PBS for 5 minutes, and incubation with blocking solution (1.5% normal goat serum in PBS) for 30 minutes at room temperature, tissue sections were incubated with anti-BrdU antibody (DAKO, Glostrup, Denmark) diluted 1:100 in PBS for 30 minutes, then with biotin-conjugated anti-mouse IgG (Vector, Burlingame, CA) diluted 1:200 in PBS for 30 minutes, followed by horseradish peroxidase (HRP)-conjugated streptavidin-biotin complex (streptABCComplex-HRP, Vectastain Elite ABC kit standard; Vector) for 1 hour at room temperature. Sections were stained in DAB-H₂O₂ (Vector) for 3 minutes and hematoxylin for 1 minute and then rinsed and covered with a coverslip. For BrdU and TUNEL double staining, Alexa568-conjugated anti-mouse IgG (1:600; Molecular Probes) was used as a secondary antibody in the BrdU staining after the TUNEL procedure. For double-staining of BrdU with Cx30 or Cx26, rabbit anti-Cx26 (1:300; Zymed Laboratories, South San Francisco, CA) or rabbit anti-Cx30 (1:400; Zymed Laboratories) antibody and anti-BrdU antibody were used as a primary antibody cocktail, and Alexa488-conjugated anti-rabbit IgG (1:400; Molecular Probes) with Alexa568-conjugated anti-mouse IgG were used as

a secondary antibody cocktail. For nuclear staining, TO-PRO-3 iodide (2 μ mol/L; Molecular Probes), 4,6-diamidino-2-phenylindole (1 μ g/ml; Dojindo Laboratories, Kumamoto, Japan) or propidium iodide (1 μ g/ml; Molecular Probes) was used. Negative controls were performed without primary antibodies to assess nonspecific binding of the secondary antibody or of the streptABC-Complex-HRP. Inner ear sections that were not injected with BrdU were also used as negative controls. Background autofluorescence was not observed in the cochlear sections with the tissue preparation methods used in the present study.

Results

Long-Term Observation of Temporary Threshold Shift and Hearing Recovery after 3NP Administration

We monitored ABR thresholds in 3NP-treated rats at 8, 20, and 40 kHz for 42 days after 3NP administration (Figure 1, A–C) to examine the potential for hearing recovery. At all frequencies, the ABR thresholds peaked 1 day after 3NP administration and then gradually recovered. At 8 kHz ($n = 7$), the threshold reached within a normal threshold level (11 dB) 42 days after 3NP administration. However, the ABR threshold at 40 kHz showed only a mild recovery after 14 days. The hearing recovery ratio, which is described in Materials and Methods, was calculated for each tested frequency (Figure 1D). At 14 days, the recovery ratios were $73.4 \pm 5.5\%$ for 8 kHz ($n = 11$), $57.0 \pm 11.2\%$ for 20 kHz ($n = 11$), and $37.5 \pm 7.7\%$ for 40 kHz ($n = 12$). At 42 days, they were $97.2 \pm 9.4\%$ for 8 kHz ($n = 7$), $67.0 \pm 16.4\%$ for 20 kHz ($n = 7$), and $32.3 \pm 7.7\%$ for 40 kHz ($n = 7$). Throughout the recovery time course, the recovery ratios at the lower frequencies always tended to be higher than those at the highest frequency. At 42 days, the recovery ratio for 8 kHz was significantly higher than that for 40 kHz ($P = 0.005$). Between 14 and 42 days after 3NP administration, the hearing level for 40 kHz did not show significant recovery, but the recovery ratios for 8 and 20 kHz showed 24 and 10% increases, respectively.

Apoptosis and Regeneration of the Cochlear Fibrocytes after 3NP Administration

To analyze the pathological changes associated with the acute hearing loss observed in the 3NP-treated rats, we performed H&E staining and TUNEL reaction to detect apoptosis. No histological changes were observed in the organ of Corti and spiral ganglion of rats with 3NP administration as shown in Figure 2, A and B. However, severe apoptosis, with chromatin condensation and apoptotic bodies, was observed only in the lateral wall and the spiral limbus at 3 days after 3NP administration (Figure 2, C and D). These severe apoptotic regions included more than 30% TUNEL-positive or apoptotic cells and were clearly demarcated as shown in Figure 2,

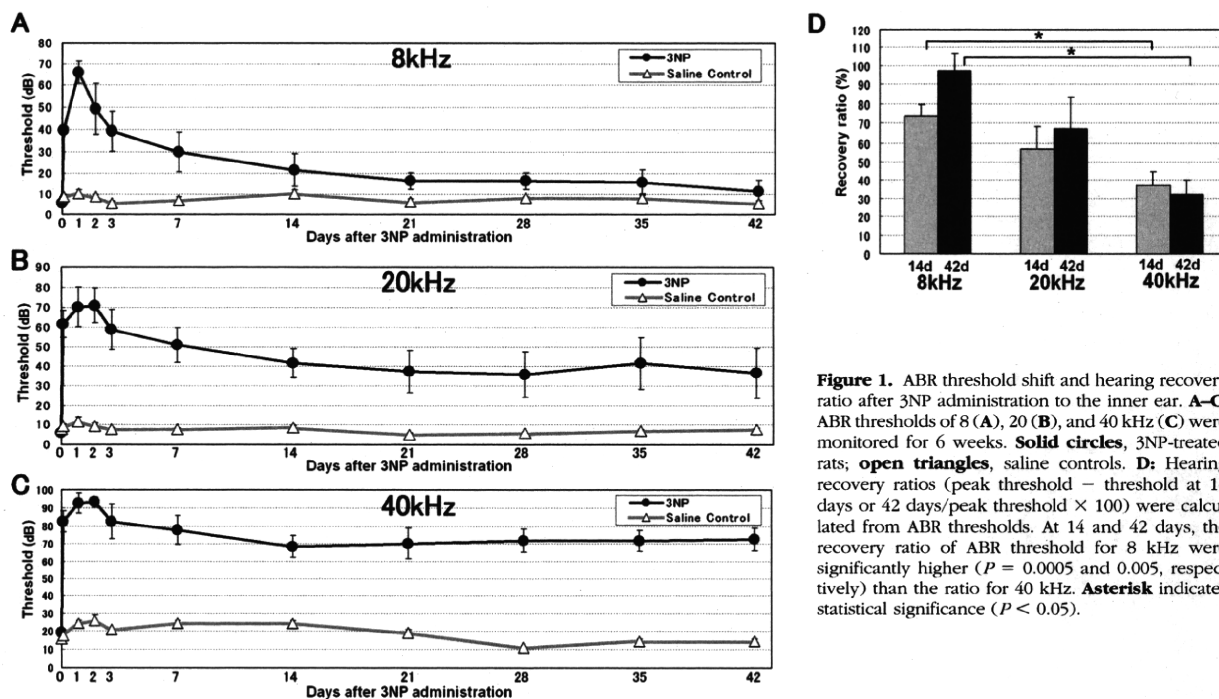


Figure 1. ABR threshold shift and hearing recovery ratio after 3NP administration to the inner ear. **A–C:** ABR thresholds of 8 (A), 20 (B), and 40 kHz (C) were monitored for 6 weeks. **Solid circles,** 3NP-treated rats; **open triangles,** saline controls. **D:** Hearing recovery ratios (peak threshold – threshold at 14 days or 42 days/peak threshold × 100) were calculated from ABR thresholds. At 14 and 42 days, the recovery ratio of ABR threshold for 8 kHz were significantly higher ($P = 0.0005$ and 0.005 , respectively) than the ratio for 40 kHz. **Asterisk** indicates statistical significance ($P < 0.05$).

E and F. These areas contain cochlear fibrocytes that participate in the potassium recycling route within the cochlea. The typical distribution pattern of TUNEL-positive cells after 3NP treatment is shown in Figure 2E, but a few rats with more severe hearing impairment (with ~55 dB elevation of the ABR threshold) demonstrated more prominent histological changes, with focal cell loss in the center surrounded by TUNEL-positive cells (Figure 2, G and H). On light microscopic observation of H&E-stained sections, histological changes suggesting inflammation were not evident in the lateral wall and spiral limbus. As for cochlear turns, lateral wall in basal turn had more severe damage than the middle turn as shown in Figure 4, G, I, and J, and the apical turn had little damage in the lateral wall.

To analyze the mechanism of hearing recovery after damage to the cochlear lateral wall, we performed a BrdU incorporation assay in addition to the TUNEL assay (Figure 3). BrdU-positive cells were observed mainly in the lateral wall fibrocytes and occasionally observed in spiral limbus, Schwann cells, and Reissner's membrane. At 3 days after 3NP administration, the BrdU-positive cell count around the area of apoptosis in the lateral wall was 6.2 ± 0.7 cells (19 cross sections from three rats) compared with 0.5 ± 0.1 cells (12 cross sections from three rats) for the control (Figure 3, A–C). Furthermore, a few TUNEL-positive dying cells that take up BrdU were detected, indicating that some fibrocytes that regenerated after 3NP administration also became apoptotic 3 days after 3NP administration (Figure 3C, arrow). To trace the cells regenerated after the early injury, the rats were continuously injected with BrdU during the first 6 days after 3NP administration and sacrificed 42 days after 3NP administration for detection of BrdU-positive cells. Few TUNEL-positive cells were detected, but a number of

BrdU-positive cells could be detected in the central part of the lateral wall in the middle turn of the cochlea (Figure 3, D–F). At 42 days after 3NP administration, 2.6 ± 0.8 BrdU-positive cells were detected in a cross section of the lateral wall of the middle turn in 3NP-treated rats (26 cross sections from five rats) compared with 0.2 ± 0.2 cells in saline-treated controls (12 cross sections from three rats). In contrast, only a few BrdU-positive cells were detected in the spiral limbus at 3 and 42 days after 3NP administration.

Characterization of MSCs

For the MSC transplantation into inner ear, we used rat bone marrow-derived cells, which we previously established and demonstrated their capacity for differentiation as MSC.²⁴ Flow cytometry of these MSCs before the transplantation demonstrated surface expression of CD29, CD44H, CD54, CD73, and CD90, but not of CD31 or CD45. This surface expression pattern was similar to human and murine MSCs.^{26,27}

Transplantation and Detection of MSCs in the Inner Ear Tissue

To improve the hearing recovery of high-frequency (40 kHz) sounds, we transplanted BrdU-labeled MSCs into the inner ear of 3NP-treated rats using perilymphatic perfusion with MSC suspension from the lateral semicircular canal. Eleven days after transplantation, a number of BrdU-positive cells were observed along the ampullary crest surface facing the perilymph in the lateral semicircular canal that was closest to the site of MSC injection (Figure 4A, arrow), suggesting that the transplanted

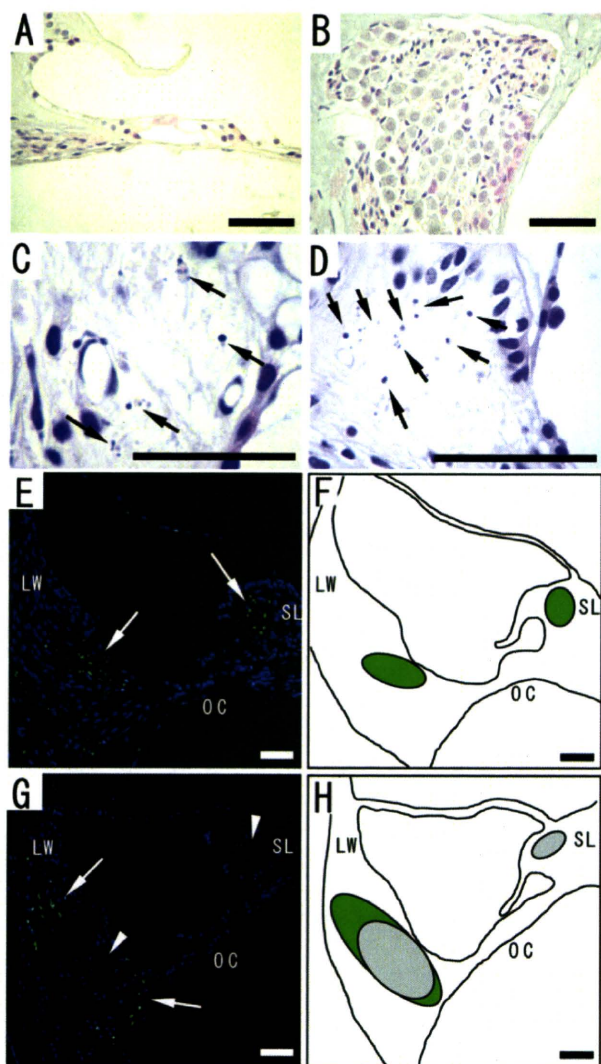


Figure 2. Apoptosis in the rat cochlea at 3 days after 3NP administration. **A–D:** H&E staining of the cochlea. Severe focal apoptosis showing chromatin condensation and apoptotic bodies (arrows) was observed in the lateral wall (C) and the spiral limbus (D), whereas no morphological changes were observed in the organ of Corti (A) and the spiral ganglion (B). **E and G:** TUNEL staining (green) of the cochlea in rats showing moderate (~35 dB elevation of ABR threshold for 8 kHz, E) and severe (~55 dB elevation of ABR threshold for 8 kHz, G) hearing impairment. **E:** The areas of apoptosis indicated by TUNEL-positive cells (arrows) were clearly demarcated in the lateral wall and spiral limbus. Nuclei were stained by TOPRO-3. **G:** Acellular areas (arrowheads) corresponded to the apoptotic areas in E, and severe apoptosis was observed in the area around the acellular site (arrows). Schematic illustration of the areas of apoptosis and cell loss in E and G are shown in F and H, respectively. Areas of apoptosis including more than 30% of TUNEL-positive cells or apoptotic cells are indicated in green, and areas of loss of fibrocytes are indicated in gray. SL, spiral limbus; LW, lateral wall; OC, organ of Corti. Scale bars = 50 μ m.

MSCs survived there even 11 days after injection. Some of these BrdU-positive cells were attached to the surface of the ampullary crest (Figure 4B, asterisk) and a number of cells had invaded the tissue (Figure 4B, arrow) although a few of the invading cells displayed morphological features suggesting rejection by the host tissue. Aggregations of MSCs were frequently observed on the bone surface in the scala tympani (Figure 4, C and D). In the apical part of the lateral wall facing the scala vestibuli, a number of BrdU-positive cells were detected within the

tissue (Figure 4E). These cells showed the morphological features of pretransplantation MSCs, ie, large and round (Figure 4F). Many BrdU-positive cells were also observed in the middle part of the lateral wall (Figure 4G) injured by 3NP treatment. The shape of these MSCs resembled that of the cochlear fibrocytes. In the hook region of the cochlea, a large number of BrdU-positive cells were also detected in the area neighboring the lateral wall injury (Figure 4, H and I). In the lateral wall of the middle turn, BrdU-positive cells were occasionally observed without a loss of fibrocytes in the corresponding area, suggesting that the MSCs that had invaded the lateral wall supplemented the injured area to repair damage (Figure 4J). In contrast to the lateral wall, only a few BrdU-positive cells were detected in the spiral limbus (Figure 4K, arrow). No morphological changes were observed in any cochlear hair cells in every group.

We used 12 3NP-treated rats and seven nontreated rats for BrdU-labeled MSC transplantation. BrdU-positive cells were detected in all of the inner ear tissues of the examined rats. Successful invasion of the lateral wall by MSCs was observed in 6 of the 12 rats treated with 3NP and one of the seven control rats (Table 1). Thus, the rats with lateral wall injury had a higher rate of MSC invasion of the lateral wall than those without injury. BrdU-positive cells were counted in five cross sections of the cochlear middle turn in each rat that showed invasion of MSCs into the lateral wall after 3NP and MSC treatment, and the approximate mean values of BrdU-positive cells observed in a cross section of the cochlear middle turn distributed between 11 and 15 in scala tympani, between 6 and 10 in apical part of lateral wall, middle part of lateral wall, and scala vestibuli, less than one in spiral limbus, and not detected in the organ of Corti and the spiral ganglion.

Expression of Gap Junction Proteins in Transplanted MSCs

To investigate the functional contribution of MSCs detected in injured and uninjured areas of the lateral wall, we analyzed expression of the gap junction proteins Cx30 and Cx26 in the transplanted MSCs. Gap junctions between cochlear fibrocytes play an important role in the cochlear potassium recycling system, and breaks in the gap junction network because of loss of fibrocytes are thought to be a main cause of the 3NP-induced hearing loss. In both normal and 3NP-treated rats, both Cx30 and Cx26 had the same expression pattern in most fibrocytes of the whole part of the lateral wall. Immunostaining for Cx30 or Cx26 showed punctuate cytoplasmic staining and strong spots of staining mainly at the sites of attachment to adjacent fibrocytes (Figure 5, A–L). All of the MSCs invaded into the lateral wall showed the expression of Cx30 and Cx26. The expression patterns of Cx30 and Cx26 in cochlear fibrocytes were the same between apical part and middle part of lateral wall, but only the invaded MSCs in the apical part of lateral wall showed different expression patterns. The MSCs detected in the apical part also expressed Cx30 and Cx26; however,

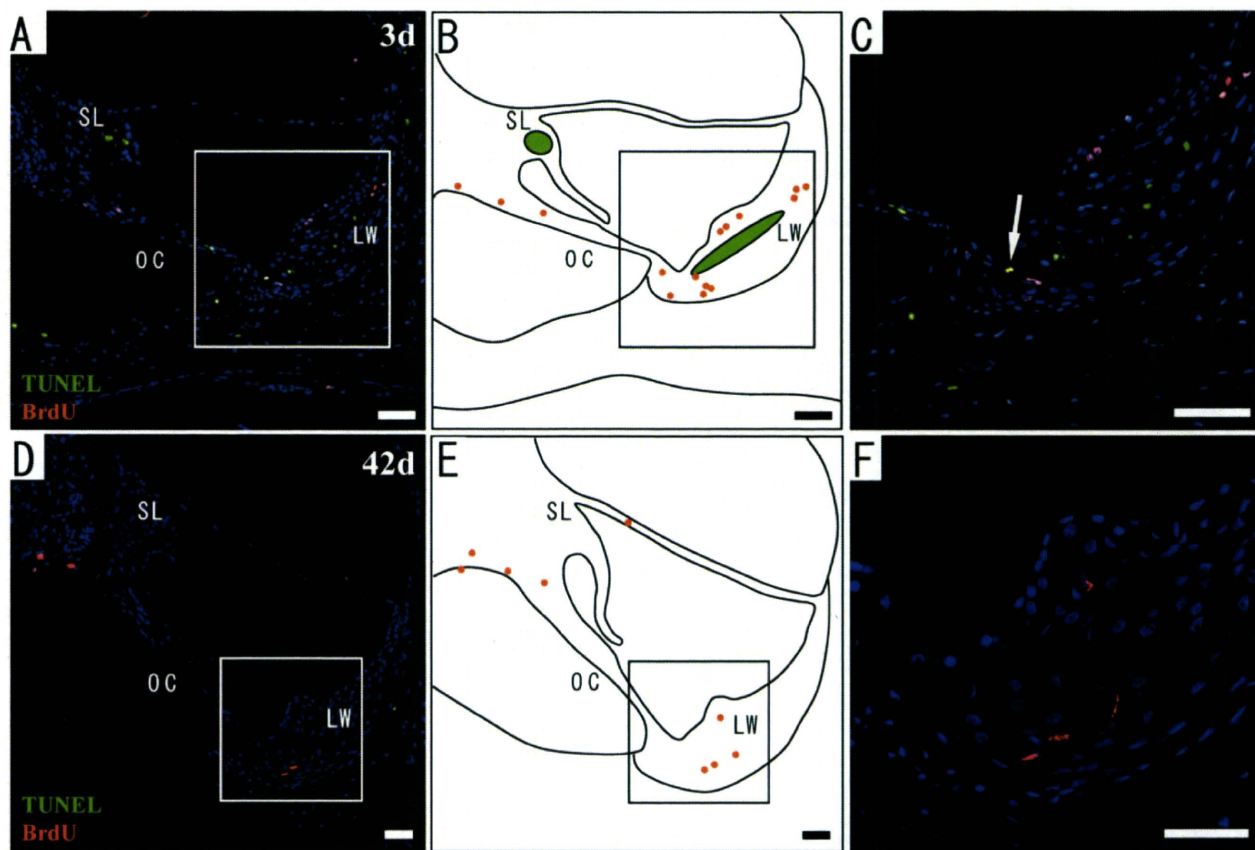


Figure 3. Regeneration and apoptosis of rat cochlear fibrocytes after 3NP administration. Double staining of BrdU (red) and TUNEL (green) assay 3 days (**A–C**) and 42 days (**D–F**) after 3NP administration. **B** and **E**: Schematic illustration for **A** and **D**. Green areas indicate the areas of apoptosis and red points indicate BrdU-positive cells. **C** and **F**: Higher magnification of the squared areas in **A** and **D**. A BrdU- and TUNEL-double-positive cell (yellow) was also observed (**arrow**). Nuclei (blue) were stained by TOPRO-3. SL, spiral limbus; LW, lateral wall; OC, organ of Corti. Scale bars = 50 μ m.

expression of Cx30 was very weak (Figure 5, A–C), and these cells did not show the punctate staining pattern at the site of contact with neighboring fibrocytes suggestive of gap junction connections (Figure 5C). Likewise, Cx26 staining spots at attachment sites to neighboring fibrocytes were not clearly observed (Figure 5, D–F). The transplanted MSCs occasionally displayed a morphology of dividing cell, suggesting that the MSCs can proliferate after their invasion into the lateral wall (Figure 5B). In contrast, within the middle part of the lateral wall near the injured region, most of the BrdU-positive cells and neighboring BrdU-negative fibrocytes strongly and similarly expressed Cx30 in the cytoplasm (Figure 5, G–I). In this area, Cx26 was also expressed by BrdU-positive cells in a similar staining pattern to BrdU-negative neighboring fibrocytes (Figure 5, J–L). BrdU-positive cells were observed even in the area where fibrocytes were not found (ie, the area without blue nuclear staining) and demonstrated Cx26 expression at the tips of their cytoplasmic processes (Figure 5, K and L; arrowheads). Moreover, these cells occasionally showed a morphology of the dividing cell (Figure 5, K and L; arrows). Nuclei of some MSCs appeared small and irregular, but signs of apoptosis such as fragmentation of nuclei were not detected in such MSCs. In addition, MSCs showed immunostaining of both Cx30 and Cx26 not only in cytoplasm and cell membrane but also in a part of nucleus, although these

proteins were not distributed in nuclei of normal cochlear fibrocytes (Figure 5, C, F, I, and L).

A summary of the histological observations shown in Figures 2, 4, and 5 and our hypothesis for the movement of transplanted MSCs are represented in the schematic illustration in Figure 6. In brief, after the perilymphatic perfusion with MSC suspension, MSCs settled on the surface of the scala tympani and the scala vestibuli within the cochlea. The injuries to cochlear fibrocytes caused by 3NP induced secretion of some chemokines from the injured area. With these stimulating signals, MSCs in the scala vestibuli invaded the lateral wall while maintaining their round shape. Then these MSCs migrated toward the injured area while maintaining the capacity for proliferation. The MSCs that reached the injured area continued to proliferate and repaired the disconnected gap junction network.

Acceleration of Hearing Recovery by MSC Transplantation

To evaluate the effect of MSC transplantation on hearing recovery in 3NP-treated rats, we monitored the ABR thresholds for 2 weeks after 3NP administration. In rats in which MSCs were transplanted without previous 3NP treatment (Figure 7, A–C), no significant threshold shift was recorded,

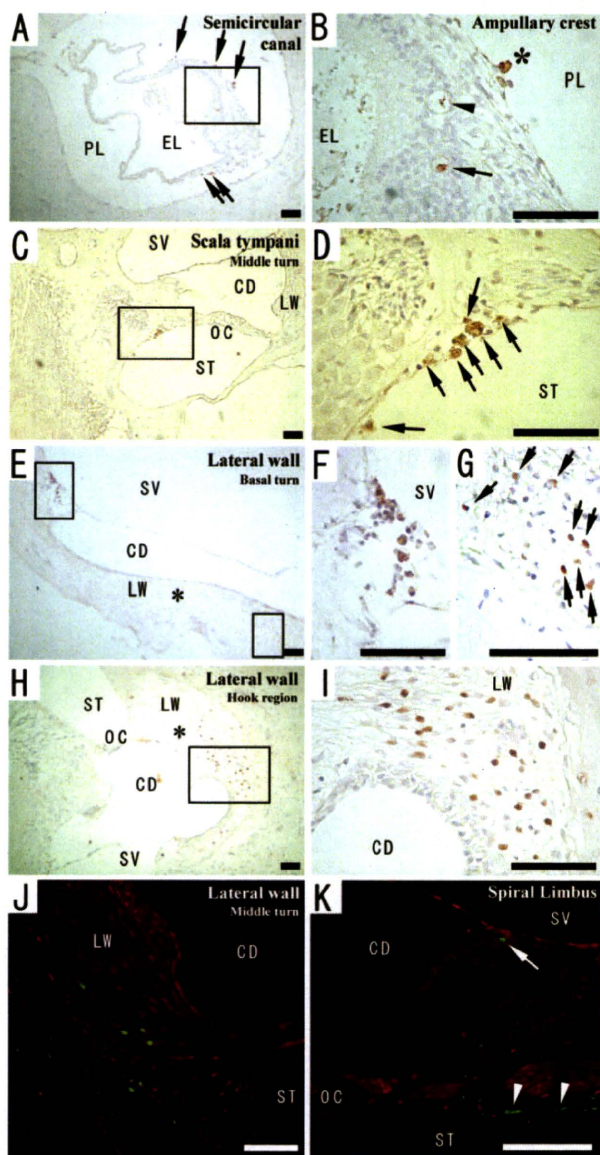


Figure 4. MSCs prelabeled with BrdU and transplanted into the inner ear of 3NP-treated rats at 11 days after the transplantation. **B, D, F, G, and I** are high-magnification images of the squared area of the left panels (**A, C, E, and H**). A number of BrdU-positive cells were observed (**A, arrows**), and some BrdU-positive cells were attached to the surface of the ampullary crest (**B, asterisk**) or had invaded the tissue (**B, arrow**). An **arrowhead** indicates BrdU-positive cells that appeared to be rejected by the recipient tissue. **C and D:** In the scala tympani, a mass of MSCs (**arrows**) was observed on the bone surface. In the cochlear lateral wall, MSCs were detected within the tissue (**E, asterisk** indicates the injured area). A number of MSCs were detected in the apical part of the lateral wall (**F**), and many MSCs were detected within the injured area of the cochlear lateral wall (**G, arrows**). **H and I:** A large number of BrdU-positive cells were detected near the injured area (**asterisk**) of the lateral wall at the hook region of the cochlea. **J and K:** Immunofluorescent staining of MSCs in the middle turn of cochlea. Only one MSC was observed in the spiral limbus (**K, arrow**). **Arrowheads** indicate MSCs that appear to be attached to the surface of the basilar membrane. Nuclei were stained with propidium iodide (red). PL, perilymph; EL, endolymph; SV, scala vestibuli; CD, cochlear duct; ST, scala tympani; LW, lateral wall; OC, organ of Corti. Scale bars = 50 μ m.

indicating that there was no significant hearing loss caused by the transplantation operation itself. Of the 12 rats that received MSC transplantation after 3NP treatment, the six rats who demonstrated MSC invasion of the lateral wall by

Table 1. Number of Rats in Which Mesenchymal Stem Cells (MSCs) Were Observed in the Cochlear Tissue 11 Days after MSC Transplantation

| | Rats tested | MSC survival | Invasion into lateral wall |
|-----------|-------------|--------------|----------------------------|
| 3NP + MSC | 12 | 12 | 6 |
| MSC only | 7 | 7 | 1 |

3NP + MSC, rats in which MSC transplantation was performed 3 days after administration of 3NP; MSC only, control rats into which MSCs were transplanted without previous 3NP administration; MSC survival, the number of rats in which surviving MSCs were detected within the cochlea; and invasion into lateral wall indicates the number of rats showing MSC invasion into the lateral wall.

histological analysis, and thus were most likely to experience recovery of hearing, were selected for ABR data collection. At 14 days after 3NP administration, the ABR thresholds both of rats receiving MSC transplantation after 3NP treatment (3NP + MSC, $n = 12$ for 8 and 20 kHz and $n = 7$ for 40 kHz) and of 3NP-treated rats that demonstrated MSC invasion of the lateral wall (3NP + MSC/LW, $n = 6$ for 8 and 20 kHz and $n = 3$ for 40 kHz) selected from 3NP + MSC in the following histochemical analysis were lower than those of 3NP-treated rats without MSC transplantation (Figure 7, A–C) for 8, 20, and 40 kHz. A remarkable decrease in the ABR threshold at 40 kHz was detected in 3NP-treated rats with MSC invasion of the lateral wall compared with the 3NP-treated group lacking transplantation at 14 days, although little difference had been seen at 7 days (Figure 7C). This result suggests that an even greater effect on the ABR threshold by MSC transplantation may be expected with a longer observation period. The 3NP-treated rats with MSC transplantation also had higher recovery ratios than the 3NP-treated rats without MSC transplantation at all tested frequencies 14 days after 3NP administration (Figure 7D). Moreover, the rats with lateral wall invasion of MSCs tended to show a higher recovery ratio than the other two groups. The difference between the 3NP-treated rats showing invasion of MSC into the lateral wall and 3NP-treated rats without transplantation was greater for higher frequencies: at 40 kHz, the recovery ratio was significantly higher ($\sim 23\%$, $P = 0.036$) for the rats with lateral wall invasion of MSCs. To examine the effect of surgical manipulation, an equal volume of vehicle (D-PBS) was also injected into the semicircular canal of 3NP-treated rats as control. These control experiments showed that the vehicle injection did not change the time course of ABR thresholds at 8 kHz but aggravated the ABR thresholds at 20 kHz at 7 days after 3NP administration and aggravated the ABR thresholds at 40 kHz at least at 7 and 14 days after 3NP administration in comparison with 3NP-treated rats with or without MSC transplantation.

Discussion

Apoptosis and Regeneration of Cochlear Fibrocytes in 3NP-Treated Rats

In this study, we demonstrated that acute hearing loss in rats treated with the mitochondrial toxin 3NP corre-

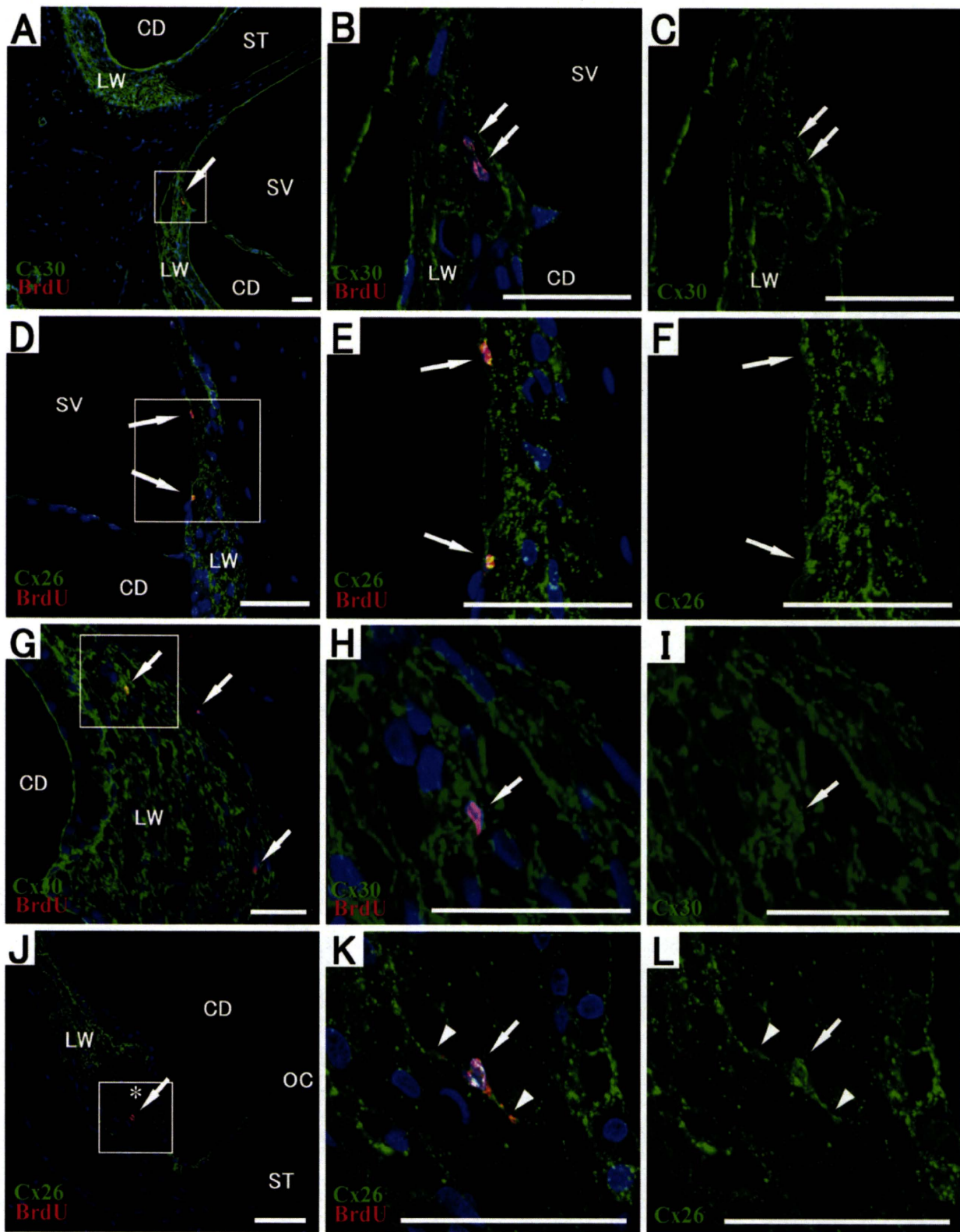


Figure 5. Expression of gap junction proteins Cx30 and Cx26 in transplanted MSCs. MSCs prelabeled with BrdU (red) are shown in the apical part (A-F) and middle part (G-L) of the lateral wall. Middle and right columns show high-magnification images of the squared area of the panels in the left column. In the right column, only Cx30 or Cx26 expression (green) is shown. A-C: In the apical part, weak expression of Cx30 was frequently detected in the BrdU-positive cells (arrows) as well as in neighboring fibrocytes. D-F: Cx26 expression was also observed in BrdU-positive cells in this area (arrows), but spots of immunostaining at cell attachment sites with neighboring fibrocytes were not visible. G-I: In the middle part of the lateral wall, strong expression of Cx30 was detected in the transplanted MSCs (arrows) as well as in neighboring fibrocytes. In this area, expression of Cx26 was observed in the MSCs even in the severely injured area (J-L, arrow). These MSCs appeared to have formed new gap junction connections (arrowheads) with neighboring fibrocytes. Nuclei were stained with 4,6-diamidino-2-phenylindole (blue). SV, scala vestibuli; CD, cochlear duct; ST, scala tympani; LW, lateral wall; OC, organ of Corti. Scale bars = 50 μ m.

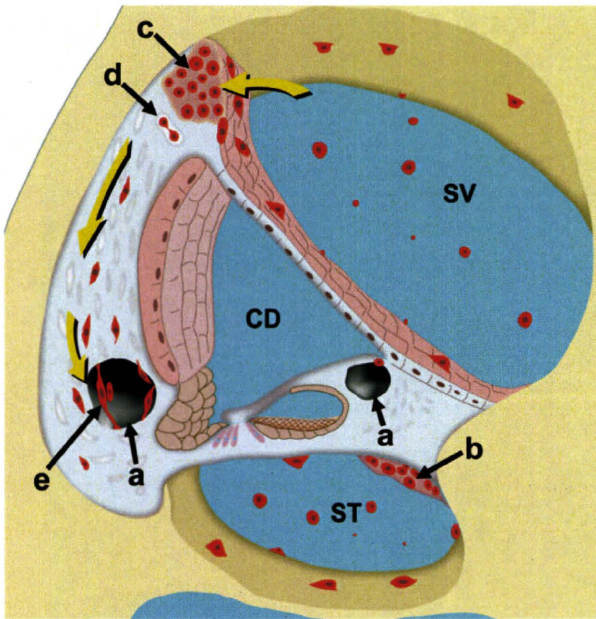


Figure 6. A summary of the histological observations shown in Figures 2, 4, and 5 and our hypothesis for the movements of the transplanted MSCs. The transplanted MSCs are represented in red. **Yellow arrows** indicate the hypothetical route of MSC migration to the injured area (**a**). Some MSCs (**b**) formed a cell mass around the scala tympani. A number of MSCs (**c**) successfully invaded the lateral wall. The invading MSCs (**d**) proliferated in the lateral wall. The MSCs that reached the injured area (**e**) continued to proliferate and repaired the disconnected gap junction network. SV, scala vestibuli; CD, cochlear duct; ST, scala tympani.

lated with a severe foci of apoptotic cochlear fibrocytes in the lateral wall and spiral limbus, both of which are indispensable to the potassium recycling system of the cochlea. The active uptake and passive conductance of K^+ by Na,K-ATPase and the gap junctions, respectively, maintain the endocochlear potential of the endolymph to generate acoustic depolarization of cochlear hair cells through a mechanically gated cation channel.²⁸ Furthermore, Na,K-ATPase is highly expressed in type II fibrocytes located lateral to the spiral prominence epithelium and suprastrial region.²⁹ In the case of a cochlear energy shortage induced by 3NP, it is assumed that the active uptake of K^+ by Na,K-ATPase would not continue but the passive conductance of K^+ via gap junctions would be maintained, resulting in an overall decrease of cytosolic $[K^+]$ in a part of the lateral wall and spiral limbus. Because potassium deprivation is a well-known cause of apoptosis,³⁰ the apoptosis of the cochlear fibrocytes we observed is likely because of low cytosolic $[K^+]$.

In the BrdU incorporation assay, active regeneration of the fibrocytes was observed near the apoptotic area in the lateral wall, suggesting that reconstruction of the potassium recycling route by cellular regeneration led to normalization of endocochlear potential and hearing recovery. Thus, regeneration of cochlear fibrocytes may be an essential process for hearing recovery after acute cochlear energy shortage (such as sudden hearing loss attributable to inner ear ischemia). These spontaneously regenerated cells are thought to be mainly generated by the mitosis of cochlear fibrocytes around the injured area.

However, the recent report suggests that bone marrow cells also have the capacity to migrate into the lateral wall and differentiate into the cochlear fibrocytes.²²

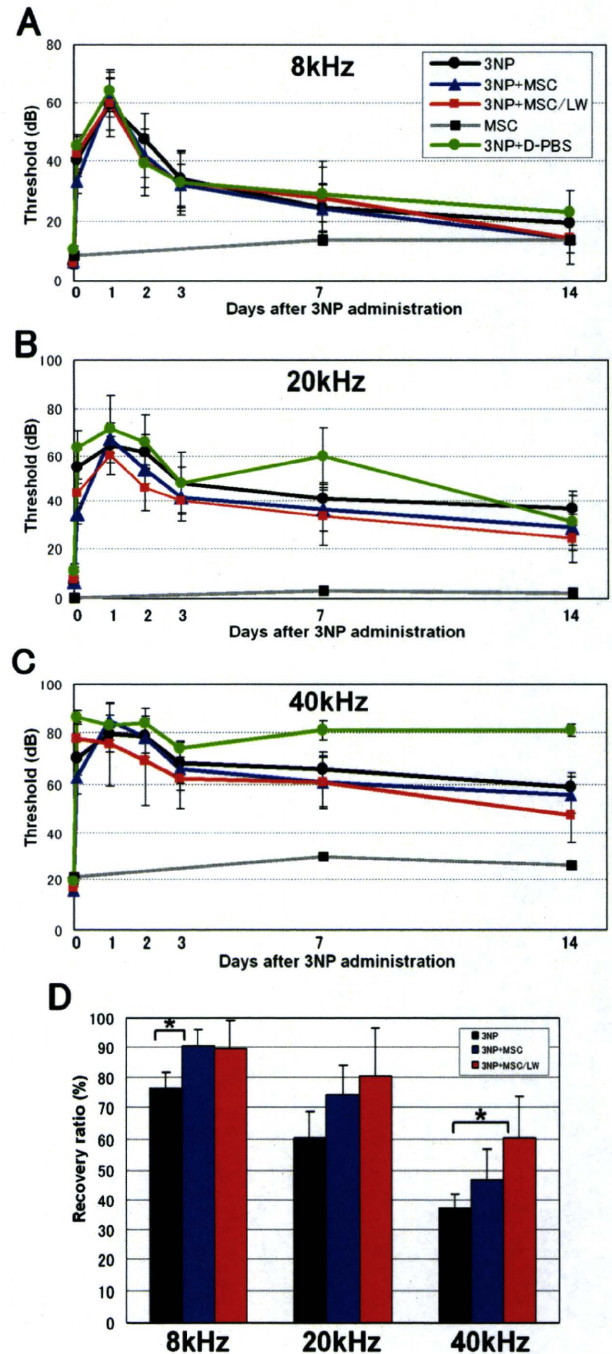


Figure 7. Hearing recovery after MSC transplantation. Thresholds of ABR for 8 (**A**), 20 (**B**), and 40 kHz (**C**) were recorded at 2 hours, 1 day, 2 days, 3 days, 7 days, and 14 days after 3NP administration. **A–C:** ABR thresholds are shown for rats with 3NP administration only (3NP, **black circle**), rats with MSC transplantation at 3 days after 3NP administration (3NP + MSC, **blue triangle**), rats with MSC transplantation at 3 days after 3NP administration and after histological confirmation of MSC invasion into the lateral wall (3NP + MSC/LW, **red square**), rats with MSC transplantation without 3NP administration (MSC, **black square**), and rats with vehicle injection (3NP + D-PBS, **green circle**). **D:** Hearing recovery ratios were calculated from ABR recovery thresholds at 2 weeks. The recovery ratios of 3NP + MSC rats (blue) and 3NP + MSC/LW rats (red) were higher than 3NP rats (black) at all frequencies. * $P < 0.05$.

Transplantation of MSCs Accelerated Hearing Recovery

The 3NP-treated rats showed complete hearing recovery at low frequencies; however, there remained a residual hearing loss at higher frequencies. Considering that the cochlear fibrocytes that were injured in this model are mesenchymal in origin, we transplanted rat MSCs into the cochlea to attempt to rescue the residual hearing loss. We used MSCs, which we previously established and demonstrated their potential as MSCs, and we further confirmed the surface antigen expression of the cells used for transplantation in flow cytometry, which showed similar expression pattern to human and murine MSCs. This suggests that the cells maintained the capacity as rat MSCs at the moment of transplantation. Because there is no barrier in the inner ear perilymph between the cochlear and vestibular compartments, cells delivered from the lateral semicircular canal by perilymphatic perfusion are considered to have reached the cochlea. Within the perilymph of the cochlea, these cells presumably spread through the scala vestibuli toward the apical turn of the cochlea, and then, after passing through the helicotrema where the scala vestibuli communicates with the scala tympani, kept moving through the scala tympani toward the basal turn. There is no other way in which MSCs can spread within the cochlear perilymph.

Our study clearly demonstrates that rat MSCs were successfully transplanted into the inner ear of 3NP-treated rats by perilymphatic perfusion from the lateral semicircular canal. A number of MSCs were detected on the surface of the ampullary crest facing the perilymph and some of them were detected within the tissue of the ampullary crest, indicating that MSCs survived at least for 11 days after the perfusion and had maintained their ability to invade and migrate into the inner ear tissue. A small number of MSCs appeared to have been rejected by the host tissue in the ampullary crest. This may be attributable to differences between the F344 and Sprague-Dawley rat strains used. In the cochlea, a number of MSCs formed cell masses on the surface of the scala tympani, where the majority of the surrounding tissue is bone tissue, suggesting that these MSCs did not invade the cochlear tissue. In the scala vestibuli, a small number of MSCs were also found attached to the surface of the bone and the Reissner membrane. However, in the apical part of the lateral wall, a number of MSCs were observed within the tissue, suggesting that MSCs had successfully invaded the lateral wall from the perilymph. This area may be an optimum site for MSC invasion.

Furthermore, some of MSCs within the tissue appeared to be undergoing mitosis and forming cell clusters, suggesting that MSCs can proliferate in the injured lateral wall to substitute for the fibrocytes lost through injury. It is likely that the MSCs that invaded the tissue from the apical part of the lateral wall migrated to the injured area in the middle part of the lateral wall. Invasion of MSCs into the lateral wall was observed in half of the rats that had 3NP treatment and MSC transplantation but in only one of seven rats that underwent only MSC transplantation,

demonstrating that rats with injury in the lateral wall had a higher rate of MSC invasion than those without injury. The approximate number of BrdU-positive cells in the whole lateral wall with 3NP treatment and MSC transplantation estimated from the immunostained cross sections is 3000 to 5000 cells in single cochlea, and it is 3 to 5% of total cells transplanted by the cell perfusion. It is known that transplanted stem cells are recruited to injury sites by chemokines.³¹ Recently, we performed DNA microarray analysis of the cochlear lateral wall RNAs in 3NP-treated rats and found a significant increase in the expression of the small inducible cytokine A2 gene encoding monocyte chemoattractant protein 1 (MCP1, data not shown), which has been reported as a chemokine that induces migration of neural stem cells.³² This may suggest that the MSC migration to the injured area of the lateral wall in this study may also be induced by chemokines because most MSCs were observed in the lateral wall in basal turn, which had a prominent damage, but not in the apical turn.

One of the most important roles of the cochlear fibrocytes is potassium ion transport for the potassium recycling system within the cochlea, and the gap junction network is essential for ion movement in this system. Thus, we analyzed the expression and distribution of the gap junction proteins Cx30 and Cx26 after MSC transplantation and found that some MSCs within the tissue in the middle part of the lateral wall showed a distribution of Cx30 and Cx26 similar to that of normal cochlear fibrocytes in the same part of the lateral wall. We also observed that MSCs that had invaded the injured area had processes that protruded toward neighboring fibrocytes with condensed Cx26 expression at the tips of the processes, suggesting that these cells invaded the injured area and reconstructed a new gap junction network with the remaining fibrocytes in the area. Moreover, these cells occasionally showed a morphology of dividing cells, suggesting that invading MSCs in the injured area could still proliferate. On the other hand, MSCs observed in the apical part of the lateral wall, which probably represented newly invading MSCs, did not show gap junction connections with their neighboring fibrocytes. The MSCs forming a cell cluster in this region had a round shape without attachments to other fibrocytes, suggesting that these MSCs may still have had stem cell potential and migratory abilities and did not contribute to ion transport. Nuclear expression of connexins in MSCs may indicate that such MSCs were not completely differentiated as cochlear fibrocytes. Nuclear expression of other connexins has been reported in the other types of cells.³³⁻³⁵ Although functional significance of nuclear expression of connexins is primarily unknown, a recent study reported that nuclear expression of connexins might exert effects on gene expression and cell growth.³⁶ In this study, invasion of the injured lateral wall by MSCs was histologically confirmed in only 50% of the treated rats, but the rate of MSC invasion of the target area could be improved by using isogenic or autologous transplantation. Otherwise, the addition of appropriate growth factors or continuous transplantation of MSCs may also improve the rates of MSC invasion.

A recent study reported that BrdU could be transferred from prelabeled grafted bone marrow cells to host neuronal precursors and glia.³⁷ Because BrdU was used to label MSCs in this study, the origin of BrdU-positive cells detected in the cochlea after MSC transplantation needs to be addressed. In the 3NP-treated rats without MSC transplantation, regenerating fibrocytes were confined around the area of apoptosis, which was clearly demarcated in the center of cochlear lateral wall. On the other hand, in the 3NP-treated rats with MSC transplantation, BrdU-positive cells were dispersed from the apical part to the central part within the lateral wall. Furthermore, morphology of BrdU-positive cells was different from neighboring fibrocytes of host tissue in both the apical part and the central part (especially in apical part as shown in Figure 4F). These findings indicate that most of BrdU-positive cells detected within the lateral wall were MSC-derived cells. However, there remains a possibility that a part of BrdU-positive cells around the area of apoptosis may be regenerating fibrocytes taking up BrdU from grafted MSCs. This question will be answered by future studies using MSCs with stable expression of green fluorescent protein by transfection of lentivirus-green fluorescent protein as donor cells.

In this study, we demonstrated that MSC transplantation into cochlea damaged by an acute energy shortage caused a significant improvement in hearing. In particular, the recovery ratio of the ABR threshold at 40 kHz was ~23% higher in the 3NP-treated rats that showed invasion of the lateral wall by MSCs than in 3NP-treated rats without MSC transplantation. This hearing recovery is thought to be caused by the supplement of fibrocytes differentiated from transplanted MSCs in the lateral wall in the basal and middle turn of cochlea. There may be an alternative possibility that the invaded MSCs induced the fibrocellular regeneration in the injured area in lateral wall. In the cochlea, the apical turn receives low-frequency sound and basal turn receives high-frequency sound such as ultrasound at least 80 kHz in rat. The cochlear region, which receives 40 kHz sound, in rat is thought to be around middle to basal turn. In this study, a number of BrdU-positive cells were found in the basal turn including the hook region, as shown in Figure 4, and this might result in the higher recovery ratio shown in 40 kHz. Without therapeutic intervention, the ABR thresholds for 40 kHz showed no improvement between 14 and 42 days after 3NP administration, suggesting that hearing loss for high-frequency sound was permanent. Thus, the MSC transplantation proved to be an effective therapy for this permanent hearing loss.

Because the vehicle injection instead of MSC suspension aggravated ABR thresholds at high frequencies, accelerated hearing recovery by MSC transplantation was considered to be induced by the effect of transplanted MSCs but not by the effect of surgical manipulation. We assume that the aggravated ABR thresholds at high frequencies may be caused by washout of secreted growth factors within the perilymph. The difference in the effects on ABR thresholds at high and low frequencies may be explained by the distinct distances from the semicircular canals where perilymphatic perfusion was

conducted. It is likely that the washout effect of perilymphatic perfusion was bigger in the high frequency area than in the low-frequency area because the high-frequency area is located closer to the semicircular canals.

Recently, stem cell transplantation directly into the inner ear has been reported in several animal experiments^{38,39}; however, data demonstrating successful improvement of hearing after these transplantations have not been reported. In addition, few reports have shown any convincing evidence that transplanted cells have invaded the injured region and repaired the structure and function. The failure to improve hearing in the previous studies may be related to the surgical methods used to deliver stem cells into the cochlea. In this study, we transplanted MSCs by cell perfusion from the lateral semicircular canal with drainage to the posterior semicircular canal to minimize the surgical effects on the cochlea. This method is similar to a recently reported technique that demonstrated the integrity of hearing function after delivery of stem cells to the inner ear⁴⁰ and confirmed that the operation produced no significant hearing defects in normal control rats.

Bone marrow MSCs have greater advantages for clinical use in human patients than other multipotential stem cells, such as embryonic stem cells because MSCs can be collected from the patient's own bone marrow for an autologous transplantation with little physical risk, no rejection risk, and few ethical problems. In the present transplantation, many MSCs were confirmed to have invaded the lateral wall and to have contributed to recovery of hearing loss despite transplantation between different rat strains. Therefore, we expect that autologous transplantation of bone marrow MSCs would be even more effective in treating hearing loss caused by injuries to the cochlear fibrocytes. In addition, significant improvement of hearing by MSC transplantation between different rat strains indicates a possibility of allogenic transplant. Even temporary effects by allogenic transplant may cause difference in the final outcome of hearing recovery by promoting regeneration or viability of host fibrocytes during acute period of injury.

This is the first report demonstrating that MSC transplantation improves incomplete hearing recovery with evidence that transplanted MSCs actually invaded the injured area and contributed to the structural reorganization of the injured cochlea. Cell therapy targeting regeneration of the cochlear fibrocytes may therefore be a powerful strategy to cure sensorineural hearing loss that cannot be reversed by current therapies.

Acknowledgments

We thank Drs. Yasuhiro Yoshikawa, Juichi Ito, Takeshi Iwata, and Yoshiyuki Ishii for their valuable help in the experiments.

References

1. Wangemann P: K⁺ cycling and the endocochlear potential. *Hear Res* 2002, 165:1-9

2. Weber PC, Cunningham III CD, Schulte BA: Potassium recycling pathways in the human cochlea. *Laryngoscope* 2001, 111:1156–1165
3. Delprat B, Ruel J, Guillon MJ, Hamard G, Lenoir M, Pujol R, Puel J-L, Brabet P, Hamel CP: Deafness and cochlear fibrocyte alterations in mice deficient for the inner ear protein otospiralin. *Mol Cell Biol* 2005, 25:847–853
4. Kikuchi T, Kimura RS, Paul DL, Adams JC: Gap junctions in the rat cochlea: immunohistochemical and ultrastructural analysis. *Anat Embryol (Berl)* 1995, 191:101–118
5. Spicer SS, Schulte BA: The fine structure of spiral ligament cells relates to ion return to the stria and varies with place-frequency. *Hear Res* 1996, 100:80–100
6. Minowa O, Ikeda K, Sugitani Y, Oshima T, Nakai S, Katori Y, Suzuki M, Furukawa M, Kawase T, Zheng Y, Ogura M, Asada Y, Watanabe K, Yamanaka H, Gotoh S, Nishi-Takeshima M, Sugimoto T, Kikuchi T, Takasaka T, Noda T: Altered cochlear fibrocytes in a mouse model of DFN3 nonsyndromic deafness. *Science* 1999, 285:1408–1411
7. Xia AP, Kikuchi T, Minowa O, Katori Y, Oshima T, Noda T, Ikeda K: Late-onset hearing loss in a mouse model of DFN3 non-syndromic deafness: morphologic and immunohistochemical analyses. *Hear Res* 2002, 166:150–158
8. Spicer SS, Schulte BA: Spiral ligament pathology in quiet-aged gerbils. *Hear Res* 2002, 172:172–185
9. Hequembourg S, Liberman MC: Spiral ligament pathology: a major aspect of age-related cochlear degeneration in C57BL/6 mice. *J Assoc Res Otolaryngol* 2001, 2:118–129
10. Wu T, Marcus DC: Age-related changes in cochlear endolymphatic potassium and potential in CD-1 and CBA/CaJ mice. *J Assoc Res Otolaryngol* 2003, 4:353–362
11. Kelsell DP, Dunlop J, Stevens HP, Lench NJ, Liang JN, Parry G, Mueller RF, Leigh IM: Connexin 26 mutations in hereditary non-syndromic sensorineural deafness. *Nature* 1997, 387:80–83
12. del Castillo I, Villamar M, Moreno-Pelayo MA, del Castillo FJ, Alvarez A, Telleria D, Menendez I, Moreno F: A deletion involving the connexin 30 gene in nonsyndromic hearing impairment. *N Engl J Med* 2002, 346:243–249
13. Hoya N, Okamoto Y, Kamiya K, Fujii M, Matsunaga T: A novel animal model of acute cochlear mitochondrial dysfunction. *Neuroreport* 2004, 15:1597–1600
14. Okamoto Y, Hoya N, Kamiya K, Fujii M, Ogawa K, Matsunaga T: Permanent threshold shift caused by acute cochlear mitochondrial dysfunction is primarily mediated by degeneration of the lateral wall of the cochlea. *Audiol Neurootol* 2005, 10:220–233
15. Alston TA, Mela L, Bright HJ: 3-Nitropropionate, the toxic substance of *Indigofera*, is a suicide inactivator of succinate dehydrogenase. *Proc Natl Acad Sci USA* 1977, 74:3767–3771
16. Coles CJ, Edmondson DE, Singer TP: Inactivation of succinate dehydrogenase by 3-nitropropionate. *J Biol Chem* 1979, 254:5161–5167
17. Brouillet E, Hantraye P, Ferrante RJ, Dolan R, Leroy-Willig A, Kowall NW, Beal MF: Chronic mitochondrial energy impairment produces selective striatal degeneration and abnormal choreiform movements in primates. *Proc Natl Acad Sci USA* 1995, 92:7105–7109
18. Hamilton BF, Gould DH: Nature and distribution of brain lesions in rats intoxicated with 3-nitropropionic acid: a type of hypoxic (energy deficient) brain damage. *Acta Neuropathol (Berl)* 1987, 72:286–297
19. Pittenger MF, Mackay AM, Beck SC, Jaiswal RK, Douglas R, Mosca JD, Moorman MA, Simonetti DW, Craig S, Marshak DR: Multilineage potential of adult human mesenchymal stem cells. *Science* 1999, 284:143–147
20. Liechty KW, MacKenzie TC, Shaaban AF, Radu A, Moseley AM, Deans R, Marshak DR, Flake AW: Human mesenchymal stem cells engraft and demonstrate site-specific differentiation after in utero transplantation in sheep. *Nat Med* 2000, 6:1282–1286
21. Jiang Y, Jahagirdar BN, Reinhardt RL, Schwartz RE, Keene CD, Ortiz-Gonzalez XR, Reyes M, Lenvik T, Lund T, Blackstad M, Du J, Aldrich S, Lisberg A, Low WC, Largaespada DA, Verfaillie CM: Pluripotency of mesenchymal stem cells derived from adult marrow. *Nature* 2002, 418:41–49
22. Lang H, Ebihara Y, Schmiedt RA, Minamiguchi H, Zhou D, Smythe N, Liu L, Ogawa M, Schulte BA: Contribution of bone marrow hematopoietic stem cells to adult mouse inner ear: mesenchymal cells and fibrocytes. *J Comp Neurol* 2006, 496:187–201
23. Kamiya K, Takahashi K, Kitamura K, Momoi T, Yoshikawa Y: Mitosis and apoptosis in postnatal auditory system of the C3H/He strain. *Brain Res* 2001, 901:296–302
24. Satoh H, Kishi K, Tanaka T, Kubota Y, Nakajima T, Akasaka Y, Ishii T: Transplanted mesenchymal stem cells are effective for skin regeneration in acute cutaneous wounds. *Cell Transplant* 2004, 13:405–412
25. Kicic A, Shen WY, Wilson AS, Constable IJ, Robertson T, Rakoczy PE: Differentiation of marrow stromal cells into photoreceptors in the rat eye. *J Neurosci* 2003, 23:7742–7749
26. Colter DC, Sekiya I, Prockop DJ: Identification of a subpopulation of rapidly self-renewing and multipotential adult stem cells in colonies of human marrow stromal cells. *Proc Natl Acad Sci USA* 2001, 98:7841–7845
27. Peister A, Mellad JA, Larson BL, Hall BM, Gibson LF, Prockop DJ: Adult stem cells from bone marrow (MSCs) isolated from different strains of inbred mice vary in surface epitopes, rates of proliferation, and differentiation potential. *Blood* 2004, 103:1662–1668
28. Corey DP, Hudspeth AJ: Ionic basis of the receptor potential in a vertebrate hair cell. *Nature* 1979, 281:675–677
29. Suko T, Ichimiya I, Yoshida K, Suzuki M, Mogi G: Classification and culture of spiral ligament fibrocytes from mice. *Hear Res* 2000, 140:137–144
30. Schuiz JB, Weller M, Klockgether T: Potassium deprivation-induced apoptosis of cerebellar granule neurons: a sequential requirement for new mRNA and protein synthesis, ICE-like protease activity, and reactive oxygen species. *J Neurosci* 1996, 16:4696–4706
31. Imitola J, Raddassi K, Park KI, Mueller J, Nieto M, Teng YD, Frenkel D, Li J, Sidman RL, Walsh CA, Snyder EY, Khoury SJ: Directed migration of neural stem cells to sites of CNS injury by the stromal cell-derived factor 1 α /CXCL chemokine receptor 4 pathway. *Proc Natl Acad Sci USA* 2004, 101:18117–18122
32. Widera D, Holtkamp W, Entschladen F, Niggemann B, Zanker K, Kaltschmidt B, Kaltschmidt C: MCP-1 induces migration of adult neural stem cells. *Eur J Cell Biol* 2004, 83:381–387
33. Eisner I, Colombo JA: Detection of a novel pattern of connexin 43 immunoreactivity responsive to dehydration in rat hypothalamic magnocellular nuclei. *Exp Neurol* 2002, 177:321–325
34. de Feijter AW, Matesic DF, Ruch RJ, Guan X, Chang CC, Trosko JE: Localization and function of the connexin 43 gap-junction protein in normal and various oncogene-expressing rat liver epithelial cells. *Mol Carcinog* 1996, 16:203–212
35. Honma S, De S, Li D, Shuler CF, Turman Jr JE: Developmental regulation of connexins 26, 32, 36, and 43 in trigeminal neurons. *Synapse* 2004, 52:258–271
36. Dang X, Doble BW, Kardami E: The carboxy-tail of connexin-43 localizes to the nucleus and inhibits cell growth. *Mol Cell Biochem* 2003, 242:35–38
37. Burns TC, Ortiz-Gonzalez XR, Gutierrez-Perez M, Keene CD, Sharda R, Demorest ZL, Jiang Y, Nelson-Holte M, Soriano M, Nakagawa Y, Luquin MR, Garcia-Verdugo JM, Prosper F, Low WC, Verfaillie CM: Thymidine analogs are transferred from prelabeled donor to host cells in the central nervous system after transplantation: a word of caution. *Stem Cells* 2006, 24:1121–1127
38. Naito Y, Nakamura T, Nakagawa T, Iguchi F, Endo T, Fujino K, Kim TS, Hiratsuka Y, Tamura T, Kanemaru S, Shimizu Y, Ito J: Transplantation of bone marrow stromal cells into the cochlea of chinchillas. *Neuroreport* 2004, 15:1–4
39. Hu Z, Wei D, Johansson CB, Holmstrom N, Duan M, Frisen J, Ulfendahl M: Survival and neural differentiation of adult neural stem cells transplanted into the mature inner ear. *Exp Cell Res* 2005, 302:40–47
40. Iguchi F, Nakagawa T, Tateya I, Endo T, Kim TS, Dong Y, Kita T, Kojima K, Naito Y, Omori K, Ito J: Surgical techniques for cell transplantation into the mouse cochlea. *Acta Otolaryngol Suppl* 2004, (551):43–47

